

The Muon Anomalous Magnetic Moment in the Excited Fermion Paradigm

M. REHMAN^{1*}, H. MUHAMMAD^{1†}, O. PANELLA^{2‡} AND M.E. GÓMEZ^{3§}

¹*Department of Physics, Comsats University Islamabad, 44000 Islamabad, Pakistan*

²*INFN, Sezione di Perugia, Via A. Pascoli, I-06123, Perugia, Italy*

³*Dpt. de Ciencias Integradas y Centro de Estudios Avanzados en Física Matemáticas y Computación, Campus del Carmen, Universidad de Huelva, Huelva 21071, Spain*

Abstract

Extensions of the Standard Model featuring excited fermions present an interesting framework that motivates the search for exotic particles at the LHC. Additionally, these extensions offer potential explanations for the muon's anomalous magnetic moment and other precision observables, shedding light on the energy scale and key parameters of the new theory. Our analysis focuses on the one-loop radiative correction originating from excited lepton doublet and triplet states using the effective Lagrangian approach. The bounds derived from the $(g - 2)_\mu$ anomaly can be complemented with the ones arising from other observables like the electroweak precision observable $\Delta\rho$ and the signals from direct LHC searches to constraint the effective theory. Our results suggest that the $(g - 2)_\mu$ anomaly can be addressed within a very narrow region of the effective theory scale. Consequently, this imposes indirect constraints on the parameter space of excited fermions.

*email: m.rehman@comsats.edu.pk

†email: hajicomats7515@gmail.com

‡email: orlando.panella@cern.ch

§email: mario.gomez@dfa.uhu.es

1 Introduction

The experimental measurements of the muon's magnetic moment $(g - 2)_\mu$ have shown a persistent and statistically significant deviation from the standard model (SM) predicted value. The latest evaluation by the Muon $g - 2$ collaboration at Fermilab [1, 2], when combined with earlier results from the Brookhaven E821 experiment [3], indicates a deviation of 5.1σ from the SM prediction [4]. The $(g - 2)_\mu$ anomaly has generated considerable interest in the scientific community as it may potentially lead to the presence of new physics beyond the SM.

Apart from the $(g - 2)_\mu$ anomaly, there are lingering questions that remain unanswered within the framework of the SM, despite its notable agreement with experimental data. Notably, the SM falls short in explaining the existence of three generations of fermions and the observed patterns in fermion masses. Answering such questions becomes feasible under the assumption of the composite structure of fermions. This presupposition entails that the SM is a limiting case of a more fundamental theory, valid up to a certain high-energy scale denoted as the composite scale Λ . The concept of compositeness predicts the existence of heavy excited particles, each corresponding to a fermion state with a mass denoted as M .

Numerous endeavors have been undertaken to explore physics at the composite scale, with a predominant focus on the production of excited fermions at colliders. Notably, studies [5, 6] concentrated on the production of excited states belonging to multiplets with isospin $I_W = 0, 1/2$. Bounds on the masses of excited fermions with $I_W = 0, 1/2$ were presented in [7, 8] based on experimental searches at the LHC. On the phenomenological front, calculations of excited fermion contributions to Z pole observables were conducted in [9] for isospin doublet states. It has been demonstrated that higher isospin multiplets up to $I_W = 1, 3/2$ are permitted by SM symmetries [10], implying the potential existence of exotic states such as quarks U^+ with a charge of $+5/3e$ and quarks D^- with a charge of $-4/3e$. Phenomenological studies exploring these exotic states have been presented in Refs. [11–14].

Experimental searches have imposed stringent constraints on the composite scale Λ and masses M of excited fermions [15–17], yet direct experimental confirmation of the existence of such states remains elusive. In the absence of direct detection, the examination of indirect effects of excited fermions on SM observables proves to be a valuable probe for understanding these states. Lately, there have been intriguing advancements in exploring the phenomenology of effective interactions of excited fermions, achieved through the computation of unitarity bounds [18]. These unitarity bounds have demonstrated significant potential when contrasted with constraints derived from direct searches at colliders [18]. Likewise, in [19], it was demonstrated that non-universal contributions to electroweak precision observables $\Delta\rho$ could considerably constrain the parameter space, particularly if the masses of the excited fermions exhibit non-degeneracy.

The effects of excited fermions with isospin doublets $I_W = 1/2$ on the muon's magnetic moment $(g - 2)_\mu$ were discussed in [20–22]. In this paper, we extend the previous work on the subject and explore effects of excited fermions with isospin doublets $I_W = 1/2$ as well as isospin triplets $I_W = 1$ on the muon's magnetic moment $(g - 2)_\mu$ at the one-loop level. The couplings of the excited fermions (leptons) of the triplet to both excited and standard fermions (leptons) were calculated using an effective field theory approach in our previous work [19], which will be detailed in Sect. 2 along with a brief description of the excited

I_W	Multiplet	Q	Y	Couple to	Couple through
0	(E^-)	-1	-2	e_R	B^μ
$\frac{1}{2}$	$\begin{pmatrix} E^0 \\ E^- \end{pmatrix}$	0 -1	-1	$\begin{pmatrix} \nu_e \\ e \end{pmatrix}_L$	B^μ, W^μ
1	$\begin{pmatrix} E^0 \\ E^- \\ E^{--} \end{pmatrix}$	0 -1 -2	-2	e_R	W^μ
$\frac{3}{2}$	$\begin{pmatrix} E^+ \\ E^0 \\ E^- \\ E^{--} \end{pmatrix}$	+1 0 -1 -2	-1	$\begin{pmatrix} \nu_e \\ e \end{pmatrix}_L$	W^μ

Table 1: Lepton multiplets for $I_W = 0, 1/2, 1, 3/2$, their charge Q , hypercharge Y and the fields through which they couple to ordinary leptons.

fermion model. The analytical outcomes for the contribution of excited fermions (leptons) to $(g-2)_\mu$ will be presented in Sect. 3. Our numerical analysis will be provided in Sect. 4, and our conclusions can be found in Sect. 5.

2 Model set-up

The majority of literature exploring the phenomenology of excited fermions typically operates under the assumption that these fermions possess $I_W = 1/2$ weak isospin. However, one can introduce the higher isospin multiplets with $I_W = 1, 3/2$ [5, 6, 23]. The coupling of these excited leptons to the gauge bosons is given by the $SU(2) \times U(1)$ invariant (and CP conserving), effective Lagrangian [9]:

$$\begin{aligned}
\mathcal{L}_{FF} = & -\bar{\Psi}^* \left[\left(g \frac{\tau^i}{2} \gamma^\mu W_\mu^i + g' \frac{Y}{2} \gamma^\mu B_\mu \right) \right. \\
& \left. + \left(\frac{g\kappa_2}{2\Lambda} \frac{\tau^i}{2} \sigma^{\mu\nu} \partial_\mu W_\nu^i + \frac{g'\kappa_1}{2\Lambda} \frac{Y}{2} \sigma^{\mu\nu} \partial_\mu B_\nu \right) \right] \Psi^*
\end{aligned} \tag{1}$$

where, we represent the excited multiplet as Ψ , with its particle composition detailed in Tab. 1. The gauge coupling constants for $SU(2)$ and $U(1)$ are denoted as g and g' , respectively, while κ_1 and κ_2 stand for dimensionless couplings. The constant Λ denotes the compositeness scale. In terms of the physical gauge fields, this can be written as:

$$\mathcal{L}_{FF} = - \sum_{V=\gamma,Z,W} \bar{F} (A_{VFF} \gamma^\mu V_\mu + K_{VFF} \sigma^{\mu\nu} \partial_\mu V_\nu) F. \tag{2}$$

where F denotes a generic excited fermion field appearing in the multiplet in Tab. 1.

The higher multiplets include states with exotic charge like doubly charged leptons. The couplings involving $I_W = 1$ excited fermions were calculated in [19] which we reproduce here for completeness. The couplings A_{VFF} are given by:

$$\begin{aligned}
A_{\gamma E^- E^-} &= -e & , & & A_{\gamma E^0 E^0} &= 0 \\
A_{\gamma E^{--} E^{--}} &= -2e & , & & A_{ZE^0 E^0} &= \frac{e}{s_W c_W} \\
A_{ZE^- E^-} &= \frac{e s_W}{c_W} & , & & A_{ZE^{--} E^{--}} &= \frac{-e(1 - 2s_W^2)}{s_W c_W} \\
A_{WE^0 E^-} &= \frac{e}{s_W} & , & & A_{WE^- E^{--}} &= \frac{e}{s_W} \\
A_{WE^0 E^{--}} &= 0 & & & &
\end{aligned} \tag{3}$$

where e represents the electric charge and c_W (s_W) are the cosine (sin) of the weak mixing angle θ_W . The couplings K_{VFF} are given by

$$\begin{aligned}
K_{\gamma E^0 E^0} &= -\frac{e}{2\Lambda}(\kappa_2 - \kappa_1) & , & & K_{\gamma E^- E^-} &= \frac{e}{2\Lambda}\kappa_1 \\
K_{\gamma E^{--} E^{--}} &= -\frac{e}{2\Lambda}(\kappa_2 + \kappa_1) & , & & K_{WE^0 E^-} &= \frac{e\kappa_2}{2\Lambda s_W} \\
K_{WE^- E^{--}} &= \frac{e}{2\Lambda s_W} & , & & K_{ZE^- E^-} &= \frac{e\kappa_1 s_W}{2\Lambda c_W} \\
K_{ZE^0 E^0} &= \frac{e(\kappa_1 s_W^2 + \kappa_2 c_W^2)}{2\Lambda c_W s_W} & , & & & \\
K_{ZE^{--} E^{--}} &= \frac{e(\kappa_1 s_W^2 - \kappa_2 c_W^2)}{2\Lambda c_W s_W} & & & &
\end{aligned} \tag{4}$$

The $SU(2) \times U(1)$ invariant dimension-five effective Lagrangian that describe the coupling of the excited fermions to the usual fermions can be written as [24]

$$\mathcal{L}_{Ff} = -\frac{1}{2\Lambda} \bar{\Psi}^* \sigma^{\mu\nu} \left(g f \frac{\tau^i}{2} W_{\mu\nu}^i + g' f' \frac{Y}{2} B_{\mu\nu} \right) \psi_L + \text{h. c.}, \tag{5}$$

where $\sigma_{\mu\nu} = (i/2)[\gamma_\mu, \gamma_\nu]$ and the dimensionless factors f and f' are presumed to be of approximately the same magnitude, around unity, and are linked to the $SU(2)$ and $U(1)$ coupling constants respectively. At tree-level, the couplings g and g' can be expressed in terms of the electric charge, e , and the Weinberg angle, θ_W , as $g = e/\sin\theta_W$ and $g' = e/\cos\theta_W$. In terms of the physical fields, the Lagrangian (5) becomes

$$\begin{aligned}
\mathcal{L}_{Ff} &= - \sum_{V=\gamma, Z, W} C_{VFf} \bar{F} \sigma^{\mu\nu} (1 - \gamma_5) f \partial_\mu V_\nu \\
&\quad - i \sum_{V=\gamma, Z} D_{VFf} \bar{F} \sigma^{\mu\nu} (1 - \gamma_5) f W_\mu V_\nu + \text{h. c.}, \tag{6}
\end{aligned}$$

where F are the excited fermion states, f the ordinary (SM) fermions and $V = \gamma, Z, W$ are the physical vector boson fields. The non-abelian structure of (5) introduces a quartic contact interaction, such as the second term in the r.h.s. of Eq. (6). In this equation, we have omitted terms containing two W bosons, which do not play any role in our calculations. For the case of $I_W = 1$ lepton multiplets, the couplings C_{VFf} and D_{VFf} can be written as

$$\begin{aligned}
C_{\gamma E^- e} &= -\frac{e}{\Lambda} f_1 & , & & C_{ZE^- e} &= -\frac{e c_W}{\Lambda s_W} f_1 \\
C_{WE^0 e} &= \frac{e}{\Lambda s_W} f_1 & , & & C_{WE^{--} e} &= \frac{e}{\Lambda s_W} f_1
\end{aligned} \tag{7}$$

Here, f_1 represents the dimensionless parameter linked to the $U(1)$ coupling constant for the triplet. The quartic interaction coupling constant, D_{VFf} , is given by

$$\begin{aligned}
D_{\gamma E^0 e} &= -D_{\gamma E^{--} e} = \frac{-e^2}{4\Lambda s_W} f_1 \\
D_{ZE^0 e} &= -D_{ZE^{--} e} = \frac{e^2 c_W}{4\Lambda s_W^2} f_1 \\
D_{WE^- e} &= \frac{-e^2}{4\Lambda s_W^2} f_1
\end{aligned} \tag{8}$$

3 Excited fermion contributions to $(g - 2)_\mu$

The contributions of excited leptons to $(g - 2)_\mu$ in the case of isospin doublets have already been studied in Ref. [22], where the evaluation of one-loop contributions to the magnetic form factors was performed using dimensional regularization technique. Utilizing the generic results presented in that study, we have derived the contributions of excited lepton triplets for the couplings specified in Eqs. (3), (4), (7), and (8). The vertex diagrams, encompassing contributions from excited lepton triplets in loops, are shown in Fig. 1, while the self-energy diagrams are shown in Fig. 2. Each Feynman diagram is associated with an excited fermion contribution denoted as Δa_μ^i , where $i = 1, 2, 3, \dots, 20$ corresponds to the respective diagram number. Employing this definition, we have

$$\Delta a_\mu^{\text{Exc}} = \sum_{i=1}^{20} \Delta a_\mu^i \tag{9}$$

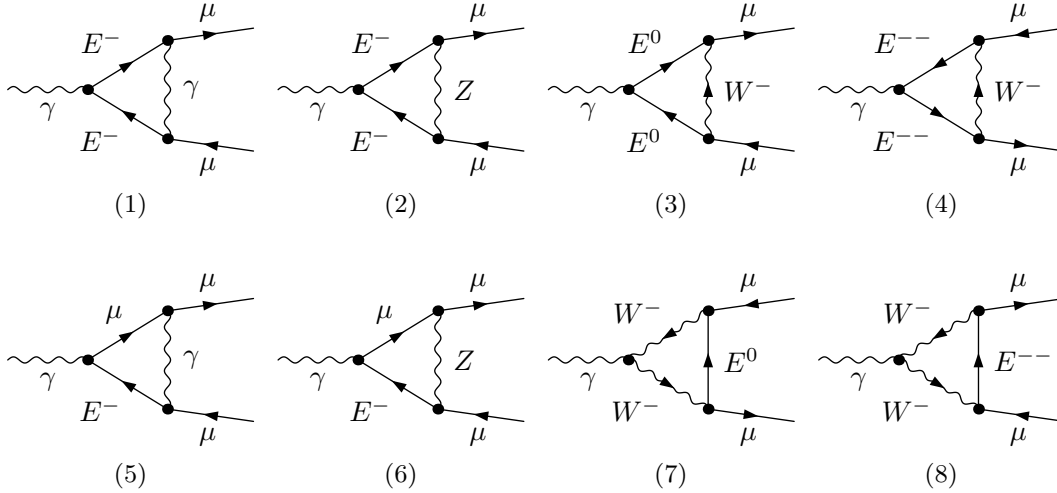


Figure 1: Vertex diagrams for the excited lepton contributions to $\Delta a_\mu^{\text{Exc}}$.

In the limit where $q^2 \ll M^2$ and considering the first order in R_Q with $R_Q = q^2/M^2$ and $R_V = M_V^2/M^2$, the corrections originating from the vertex diagrams shown in Fig. 1 can be expressed as

$$\Delta a_\mu^1 = \frac{1}{36\pi} \frac{m_\mu^2 \alpha}{\Lambda^2} f_1^2 \left[120 - 108 \left(\frac{M}{2\Lambda} \right) k_1 + 72 \left(-1 + \left(\frac{M}{2\Lambda} \right) k_1 \right) \log \frac{\Lambda^2}{M^2} \right] \quad (10)$$

$$\Delta a_\mu^2 = \frac{1}{36\pi} \frac{m_\mu^2 \alpha}{\Lambda^2} f_1^2 \frac{C_W^2}{S_W^2} \left[6(20 + 9R_Z) - 36 \left(\frac{M}{2\Lambda} k_1 \right) (3 + R_Z) + 72 \left(-1 + \left(\frac{M}{2\Lambda} k_1 \right) \right) \log \frac{\Lambda^2}{M^2} \right] \quad (11)$$

$$\Delta a_\mu^3 = \frac{1}{36\pi} \frac{m_\mu^2 \alpha}{\Lambda^2 S_W^2} f_1^2 \left[36 \left(\frac{M}{2\Lambda} \right) (k_2 - k_1) (3 + R_W) - 72 \left(\frac{M}{2\Lambda} \right) (k_2 - k_1) \log \frac{\Lambda^2}{M^2} \right] \quad (12)$$

$$\Delta a_\mu^4 = \frac{1}{36\pi} \frac{m_\mu^2 \alpha}{\Lambda^2 S_W^2} f_1^2 \left[12(20 + 9R_W) + 36 \left(\frac{M}{2\Lambda} \right) (k_2 + k_1) (3 + R_W) - 72 \left(2 + \left(\frac{M}{2\Lambda} \right) (k_2 + k_1) \right) \log \frac{\Lambda^2}{M^2} \right] \quad (13)$$

$$\Delta a_\mu^5 = \frac{1}{2\pi} \frac{m_\mu^2 \alpha}{\Lambda^2} f_1^2 \left[1 + 2 \log \frac{\Lambda^2}{M^2} \right] \quad (14)$$

$$\Delta a_\mu^6 = \frac{-1}{24\pi} \left(\frac{m_\mu^2 \alpha}{\Lambda^2 S_W} \right) f_1^2 \left[(4S_W^2 - 1)(3 + 6R_Z + 12R_Z \log R_Z + 6 \log \frac{\Lambda^2}{M^2}) - (39 + 6R_Z + 12R_Z \log R_Z + 6 \log \frac{\Lambda^2}{M^2}) \right] \quad (15)$$

$$\Delta a_\mu^7 = \Delta a_\mu^8 = \frac{1}{36\pi} \frac{m_\mu^2 \alpha}{\Lambda^2 S_W} f_1^2 \left[-79 - 120R_W + 42 \log \frac{\Lambda^2}{M^2} \right] \quad (16)$$

where m_μ represents the mass of the muon and α denotes the fine-structure constant.

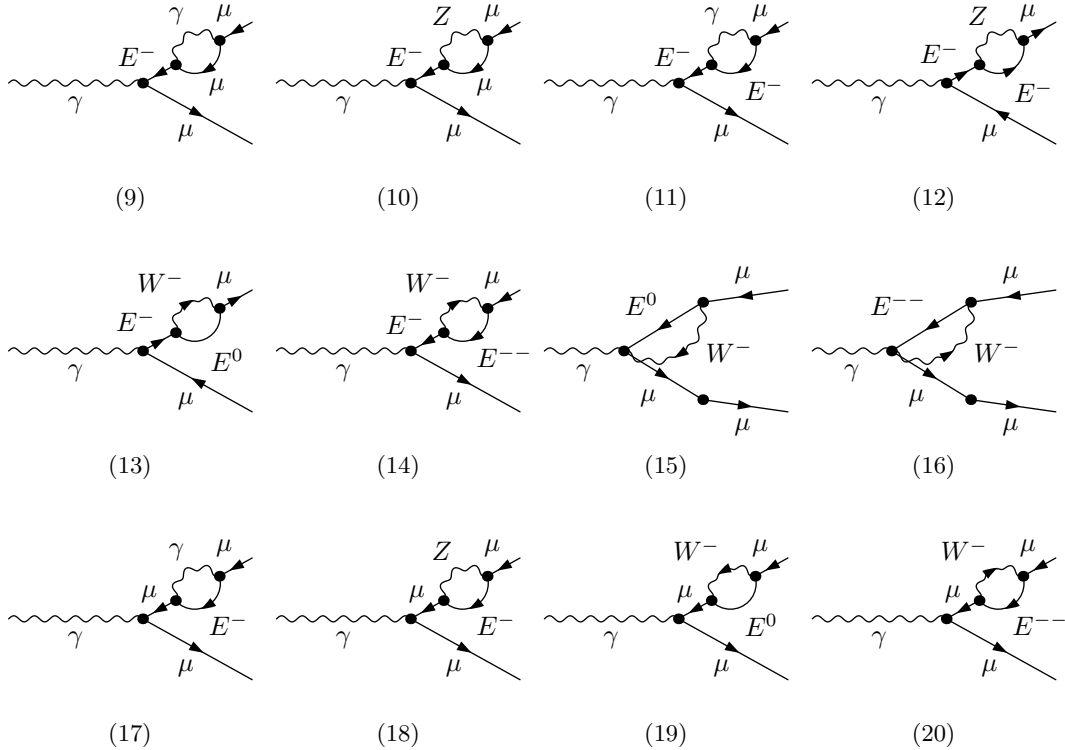


Figure 2: Self-energy diagrams for the excited lepton contributions to $\Delta a_\mu^{\text{Exc}}$.

Under the previously specified limit, the approximate corrections to $\Delta a_\mu^{\text{Exc}}$, considering the first order in R_Q , arising from the self-energy diagrams presented in Fig. 2, can be written as

$$\Delta a_\mu^9 = \frac{2}{\pi} \frac{m_\mu^2 \alpha}{\Lambda^2} f_1^2 \left(\frac{\Lambda^2}{M^2} \right) \quad (17)$$

$$\Delta a_\mu^{10} = \frac{-1}{\pi} \frac{m_\mu^2 \alpha}{\Lambda^2 S_W^2} f_1^2 (2S_W^2 - 1) \left(2R_Z + 3R_Z \log R_Z - 3R_Z \log \frac{\Lambda^2}{M^2} + \frac{\Lambda^2}{M^2} \right) \quad (18)$$

$$\Delta a_\mu^{11} = \frac{1}{2\pi} \frac{m_\mu^2 \alpha}{\Lambda^2} f_1^2 \left[\begin{array}{c} 15 - 22(\frac{M}{2\Lambda} k_1) + 6(-3 + 4(\frac{M}{2\Lambda} k_1)) \log \frac{\Lambda^2}{M^2} \\ -4 \frac{\Lambda^2}{M^2} (-1 + (\frac{M}{2\Lambda} k_1)) \end{array} \right] \quad (19)$$

$$\Delta a_\mu^{12} = \frac{-1}{2\pi} \frac{m_\mu^2 \alpha}{\Lambda^2} f_1^2 \left[\begin{array}{c} 15 + 14R_Z + (\frac{M}{2\Lambda} k_1)(22 + 21R_Z) \\ -6(3 + 2R_Z + (\frac{M}{2\Lambda} k_1)(4 + 3R_Z)) \log \frac{\Lambda^2}{M^2} \\ +4 \frac{\Lambda^2}{M^2} (1 + (\frac{M}{2\Lambda} k_1)) \end{array} \right] \quad (20)$$

$$\Delta a_\mu^{13} = \frac{1}{2\pi} \frac{m_\mu^2 \alpha}{S_W^2 \Lambda^2} f_1^2 \left[\begin{array}{c} 15 + 14R_W + (\frac{M}{2\Lambda} k_2)(22 + 21R_W) \\ -6(3 + 2R_W + (\frac{M}{2\Lambda} k_2)(4 + 3R_W)) \log \frac{\Lambda^2}{M^2} \\ +4 \frac{\Lambda^2}{M^2} (1 + (\frac{M}{2\Lambda} k_2)) \end{array} \right] \quad (21)$$

$$\Delta a_\mu^{14} = \frac{1}{2\pi} \frac{m_\mu^2 \alpha}{S_W^2 \Lambda^2} f_1^2 \left[\begin{array}{c} 15 + 14R_W + (\frac{M}{2\Lambda})(22 + 21R_W) \\ -6(3 + 2R_W + (\frac{M}{2\Lambda})(4 + 3R_W)) \log \frac{\Lambda^2}{M^2} \\ +4 \frac{\Lambda^2}{M^2} (1 + (\frac{M}{2\Lambda})) \end{array} \right] \quad (22)$$

$$\Delta a_\mu^{15} = -\Delta a_\mu^{16} = \frac{1}{36\pi} \frac{m_\mu^2 \alpha}{S_W^2 \Lambda^2} f_1^2 \left(1 + 12R_W - 6 \log \frac{\Lambda^2}{M^2} \right) \quad (23)$$

$$\Delta a_\mu^{17} = \Delta a_\mu^{18} = \Delta a_\mu^{19} = \Delta a_\mu^{20} = 0 \quad (24)$$

The results presented above are obtained with the assumption that the masses of the excited leptons are degenerate.

4 Numerical Results

Considerable attention has been directed toward the longstanding anomaly observed in the value of $(g-2)_\mu$. The most recent assessment, undertaken by the Run II and Run III of the Muon $g-2$ collaboration at Fermilab [1], when combined with earlier findings from the same experiment [2] and the Brookhaven E821 experiment [3], reveals a deviation of 5.1σ from the SM prediction¹ [4, 25].

$$\Delta \alpha_\mu = \alpha_\mu^{\text{exp}} - \alpha_\mu^{\text{SM}} = (24.9 \pm 4.8) \times 10^{-10}. \quad (25)$$

The essential parameters for defining the effective theory include the energy scale Λ , the mass range of exotic particles denoted by M , and the dimensionless factors κ_1 , κ_2 , f' , f and f_1 . The factors f' and f are involved in the doublet calculations, whereas the parameter f_1 pertains to triplets. For our numerical evaluation, we examined the value of Λ within the interval $0 < \Lambda < 25$ GeV and M within the range $0 < M < 12$ GeV. However, κ_1 and κ_2 are

¹The latest announcement from the CMD-3 collaboration [26] brings a refinement to the $(g-2)_\mu$ anomaly, narrowing it down to just 1σ . However, their results deviate from all previous measurements, and the underlying reason for this inconsistency remains unresolved. Consequently, this poses a challenge to achieving a conclusive comparison between experimental results and SM predictions for $(g-2)_\mu$ [27].

set to unity since their influence on our calculations is negligible. Yet, we've observed that while f' , f and f_1 are inconsequential for $\Delta\rho$, they can significantly affect the computation of $\Delta\alpha_\mu$. We investigate two cases for f' and f : one assumes equal values, denoted as $f' = f$, while the other examines various combinations for f' and f .

Considering that excited fermion masses typically emerge above the Electroweak Symmetry Breaking (EWSB) scale, we can presume they have similar magnitudes. However, our previous work [19] highlighted $\Delta\rho$'s sensitivity to doublet and triplet mass non-degeneracy. Although $\Delta\alpha_\mu$ is not affected by this, it's advantageous to allow for such possibilities to integrate constraints from both $\Delta\alpha_\mu$ and $\Delta\rho$. Hence, we incorporate the potential for slight mass differences among exotic fermions within the same isospin multiplet, which may arise from SU(2) breaking contributions such as interactions with exotic Higgs bosons.

4.1 Contributions to $(g-2)_\mu$ from degenerate Fermion Masses with $f' = f$

Utilizing the formulas provided in Eqs. (11-24), we can estimate $\Delta a_\mu^{\text{Exc}}$. Our results for doublet contributions are presented in Fig. 3, while triplet contributions are illustrated in Fig. 4, showcasing contours of $\Delta a_\mu^{\text{Exc}}$ in the (M, Λ) plane. Additionally, these figures incorporate experimental findings, indicating exclusion regions in the (M, Λ) plane with a 95% confidence level [15–17]. The dashed blue line corresponds to the recent CMS search for an excited lepton decaying to two muons and two jets via contact interaction, with a total integrated luminosity of 139 fb^{-1} , the orange line corresponds to the search in the $\ell\ell\gamma$ channel with an integrated luminosity of 35.9 fb^{-1} and the red line corresponds to recent ATLAS search in the $\tau\tau jj$ channel with an integrated luminosity of 139 fb^{-1} . Perturbative unitarity bounds for a composite fermion model were explored in [18], with the purple line representing these bounds, and the decreasing thickness of the line corresponding to 100%, 95%, and 50% event fractions, respectively, that satisfy unitarity bounds. The shaded area is excluded due to unitarity bounds (purple lines) and direct searches at the LHC (blue, orange and red lines).

The contours of $\Delta a_\mu^{\text{Exc}}$ for various values of the weight factor f , associated with the SU(2) and U(1) couplings of the excited fermion to ordinary fermions, are depicted in Fig. 3. The dashed black line represents the central value of Δa_μ as given in Eq. (25), while the yellow, green, and pink regions denote the 1σ , 2σ , and 3σ regions, respectively. The upper-left (upper-right) plot corresponds to a value of weight factor $f = 10$ ($f = 20$), whereas the lower-left (lower-right) plot corresponds to $f = 30$ ($f = 40$).

The plots reveal the high sensitivity of $\Delta a_\mu^{\text{Exc}}$ to the chosen value of the weight factor f . For smaller values such as $f = 10$, the doublet contributions are minimal and largely fall within regions already excluded by experimental searches and/or unitarity bounds. However, for larger values of f , such as $f = 20$, the required value of $\Delta a_\mu^{\text{Exc}}$ can be achieved in regions that are still permitted by experimental searches and unitarity bounds. For the values greater than $f = 30$, the required value of $\Delta a_\mu^{\text{Exc}}$ lies in the allowed region however, the band depicting the 1σ , 2σ , and 3σ regions get shrunk to a minimum.

Our results for the triplet contribution are presented in Fig. 4. In this figure, the upper-left (upper-right) plot corresponds to a value of weight factor $f_1 = 3$ ($f_1 = 5$), while the lower-left (lower-right) plot corresponds to $f_1 = 7$ ($f_1 = 10$). The shading of contours follows the same convention as in the previous figure. For $f_1 = 3, 5$, the required value of $\Delta a_\mu^{\text{Exc}}$ pre-

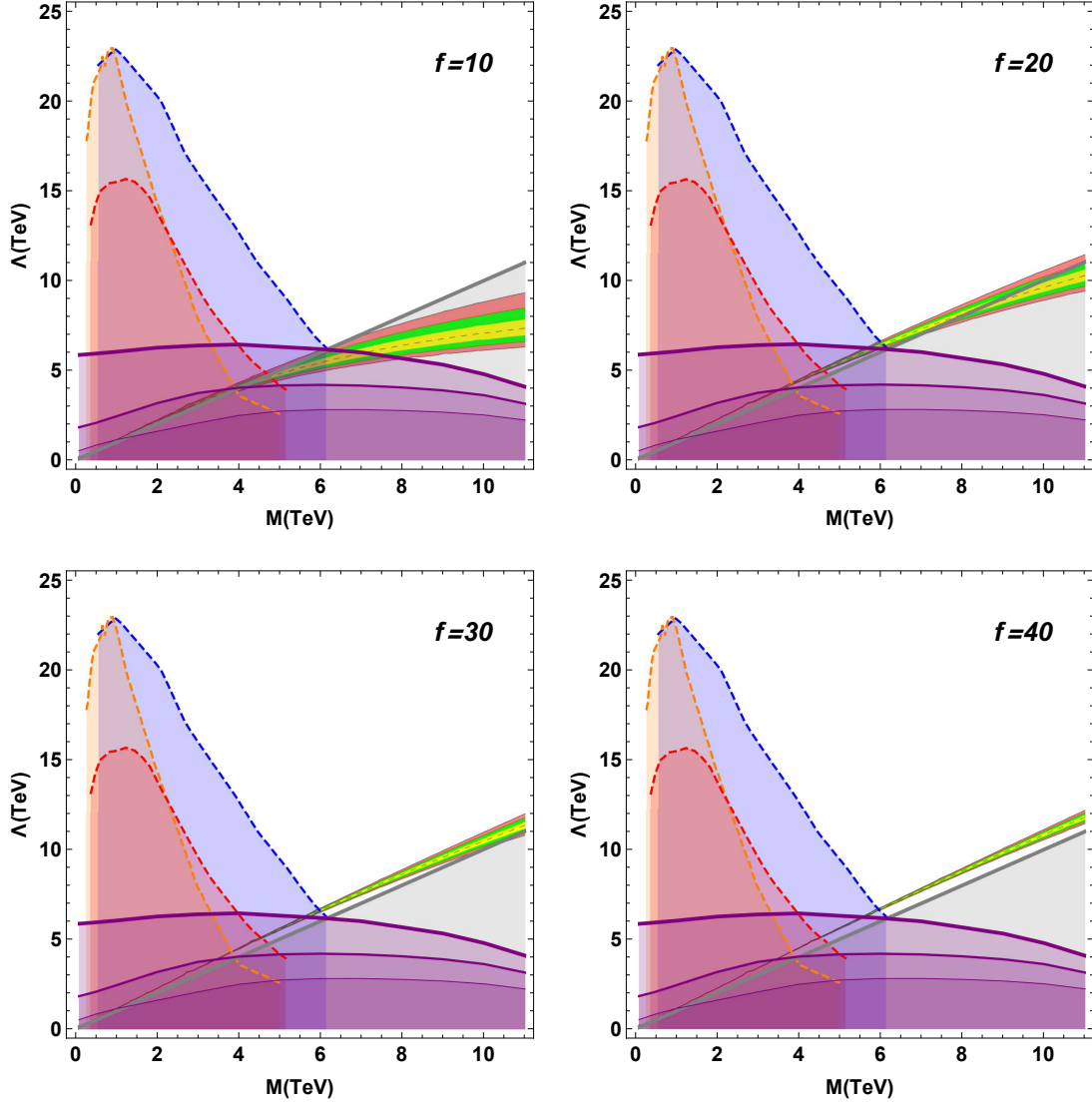


Figure 3: $\Delta a_\mu^{\text{Exc}}$ in (M, Λ) plane for the case of excited lepton doublet. The upper-left (upper-right) plot corresponds to the value of weight factor $f = 10$ ($f = 20$) whereas the lower-left (lower-right) plot correspond to the value $f = 30$ ($f = 40$). The dashed black line represents the central value of Δa_μ as given in Eq. (25), while the yellow, green, and pink regions denote the 1σ , 2σ , and 3σ regions, respectively. $M = \Lambda$ line (solid gray), unitarity bound (purple lines) [18] and exclusion limits (blue, orange and red dashed lines) [15–17] from CMS and ATLAS experiments for charged leptons searches with two different final states are also shown for comparison.

dominantly lies in regions already excluded. However, for larger values of f_1 , i.e., $f_1 = 7, 10$, the required value of $\Delta a_\mu^{\text{Exc}}$ can be achieved in regions that are still permissible according to experimental searches and unitarity bounds. It is noteworthy that triplet contributions are relatively more significant than doublet contributions for the same value of f_1 .

In summary, for both doublet and triplet contributions, the explanation of the $(g - 2)_\mu$

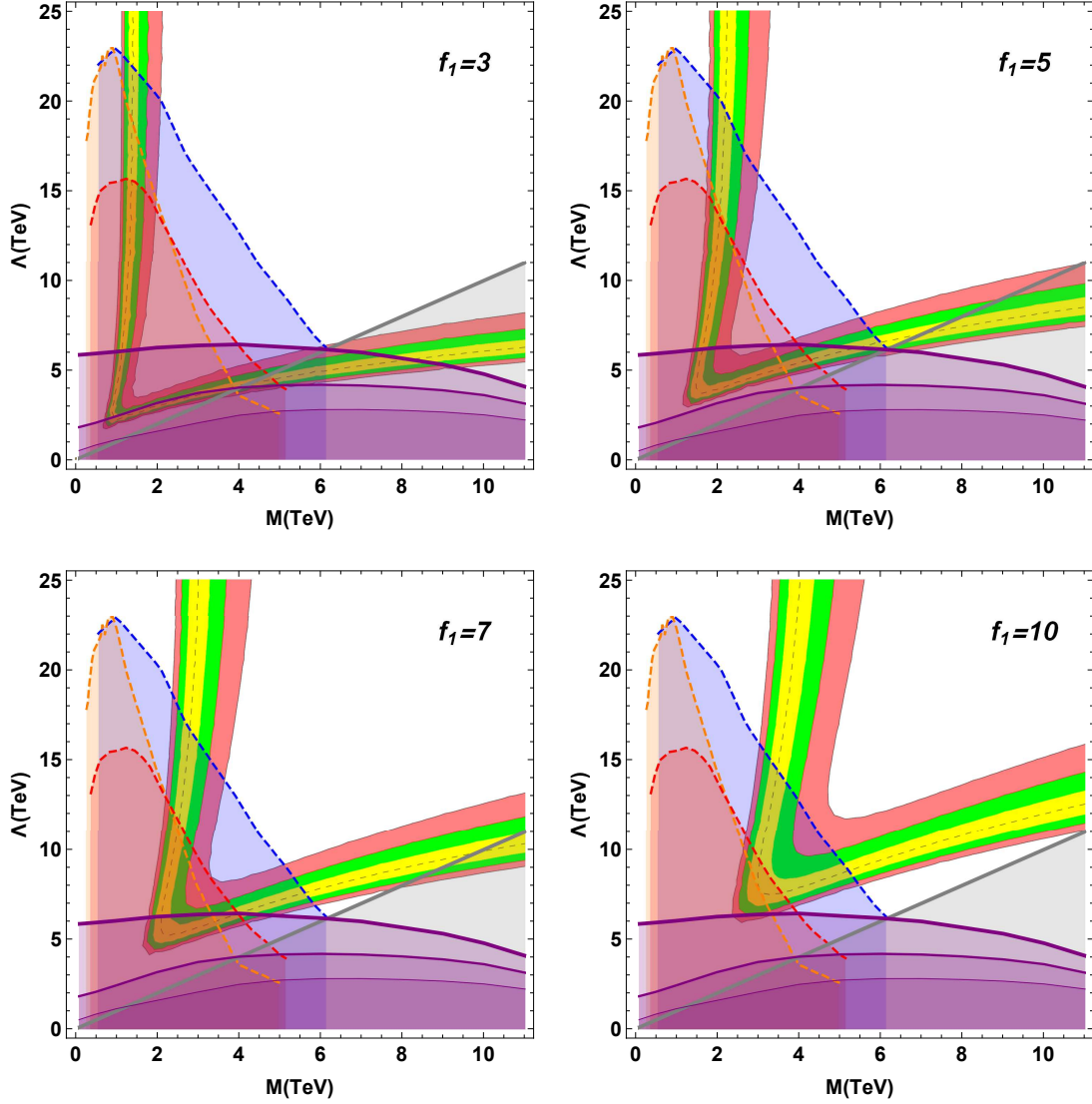


Figure 4: $\Delta a_\mu^{\text{Exc}}$ in (M, Λ) plane for the case of excited lepton triplet. The upper-left (upper-right) plot corresponds to the value of weight factor $f_1 = 3$ ($f_1 = 5$) whereas the lower-left (lower-right) plot correspond to the value $f_1 = 7$ ($f_1 = 10$). Lines and color coding remain same as in previous figure.

anomaly is feasible only within a highly restricted area of the (M, Λ) plane. This limitation serves as an indirect constraint on the parameter space.

4.2 Contributions to $(g-2)_\mu$ from degenerate Fermion Masses with $f' \neq f$

In the literature, it is usually assumed that the weight factors associated with $SU(2)$ and $U(1)$ couplings are equal i.e. $f' = f$. In theory, they can indeed differ. In triplet calculations, only f_1 is involved, thus yielding unchanged results. Conversely, for doublets, both factors

f' and f hold significance. In this section, we explore the cases where $f' \neq f$.

In Fig. 5, we present our findings for $\Delta a_\mu^{\text{Exc}}$ plotted in the (M, Λ) plane for the excited lepton doublet, considering four combinations of f' and f . The plots in the upper-left and upper-right correspond to $f' = -10, f = 1$ and $f' = -10, f = 5$ respectively, while the lower-left and lower-right plots correspond to $f' = -20, f = 1$ and $f' = -20, f = 5$ respectively. While the possibility of selecting negative values for f exists, we have checked that it has minimal impact on the results. Conversely, selecting a negative value for f' leads to drastic changes as can be seen in the Fig. 5. In this case, it is possible to obtain the required value of $(g - 2)_\mu$ within the allowed range of parameter space for the doublet contributions. Furthermore, relatively small values of f' and f can explain the $(g - 2)_\mu$ anomaly, contrasting with the previous case where higher values were required.

4.3 Contributions to $(g - 2)_\mu$ for the case of non-degenerate fermion masses

Here, we expand our analysis to investigate the impacts of non-degenerate excited fermions entering via $\Delta\rho$. For the doublet contributions with $f' = f$, we show our results in Figs. 6-7. As shown in Fig. 6, the required value of $(g - 2)_\mu$ remains in the allowed region if $\delta M < 15$ GeV (dotted-dashed black line), where δM denote the mass difference between the excited fermion species. However, for $\delta M > 15$ GeV (refer to (dotted-dashed black line) in Fig. 7), the $(g - 2)_\mu$ anomaly cannot be accounted for, as the requisite $\Delta a_\mu^{\text{Exc}}$ value falls within the region excluded by $\Delta\rho$. We also examined cases where $f' \neq f$. Nevertheless, the required $(g - 2)_\mu$ value remains within the allowed range and is not affected by the $\Delta\rho$ constraints.

Concerning the contributions from triplets, our results are displayed in Figs. 8-9. Here, for $\delta M < 10$ GeV (dotted-dashed black line), there exists a parameter space where the $(g - 2)_\mu$ anomaly is explainable. However, for $\delta M > 10$ GeV, the $(g - 2)_\mu$ anomaly cannot be rationalized except in a very narrow region for $f_1 = 10$ (refer to lower-right plot in Fig. 9), as the required $\Delta a_\mu^{\text{Exc}}$ value mostly falls within the region excluded by $\Delta\rho$.

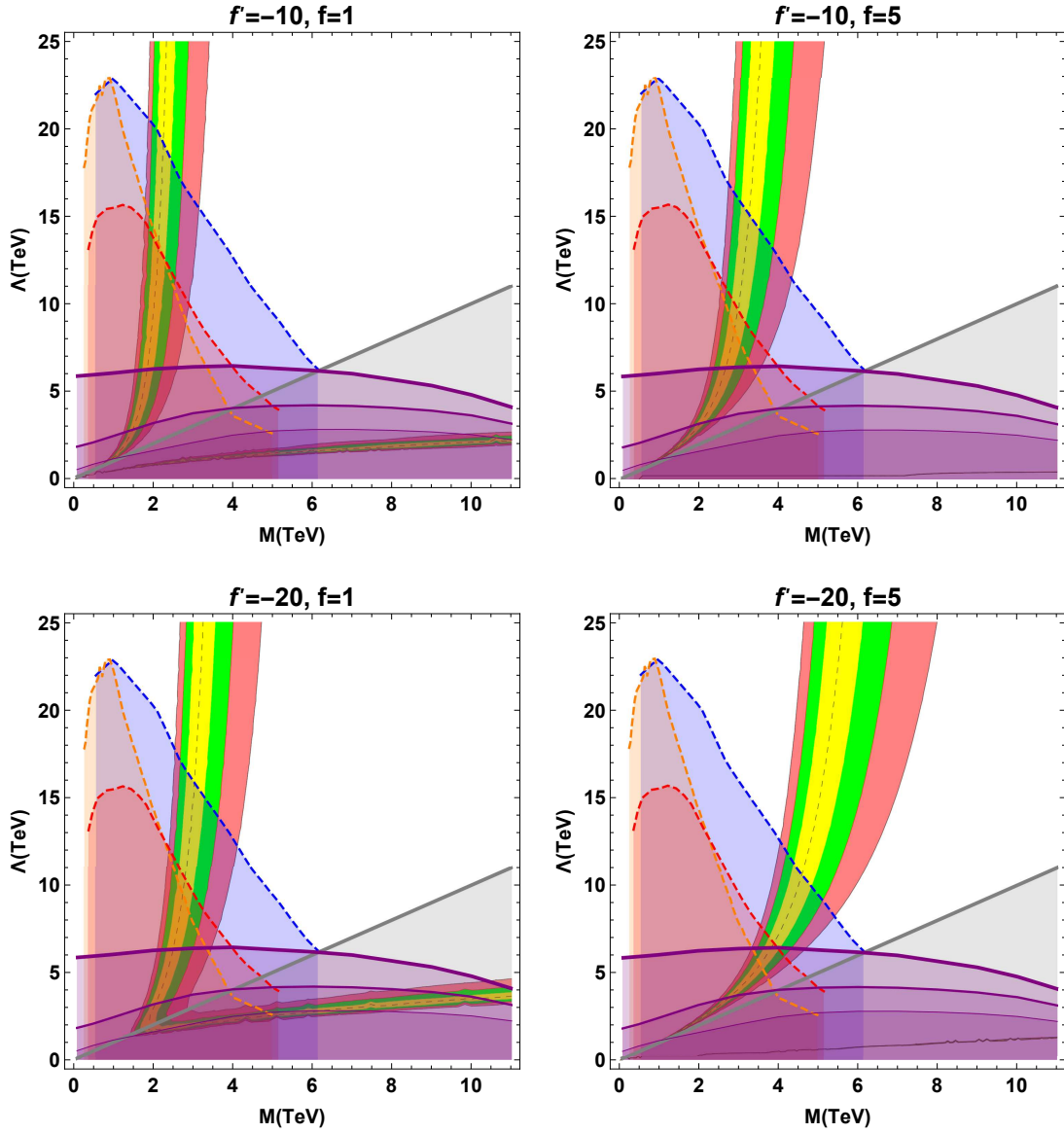


Figure 5: $\Delta a_{\mu}^{\text{Exc}}$ in (M, Λ) plane for the case of excited lepton doublet. The upper-left (upper-right) plot corresponds to the value of weight factor $f' = -10, f = 1$ ($f' = -10, f = 5$) whereas the lower-left (lower-right) plot correspond to the value $f' = -20, f = 1$ ($f' = -20, f = 5$). Other lines and color coding remain same as in previous figures.

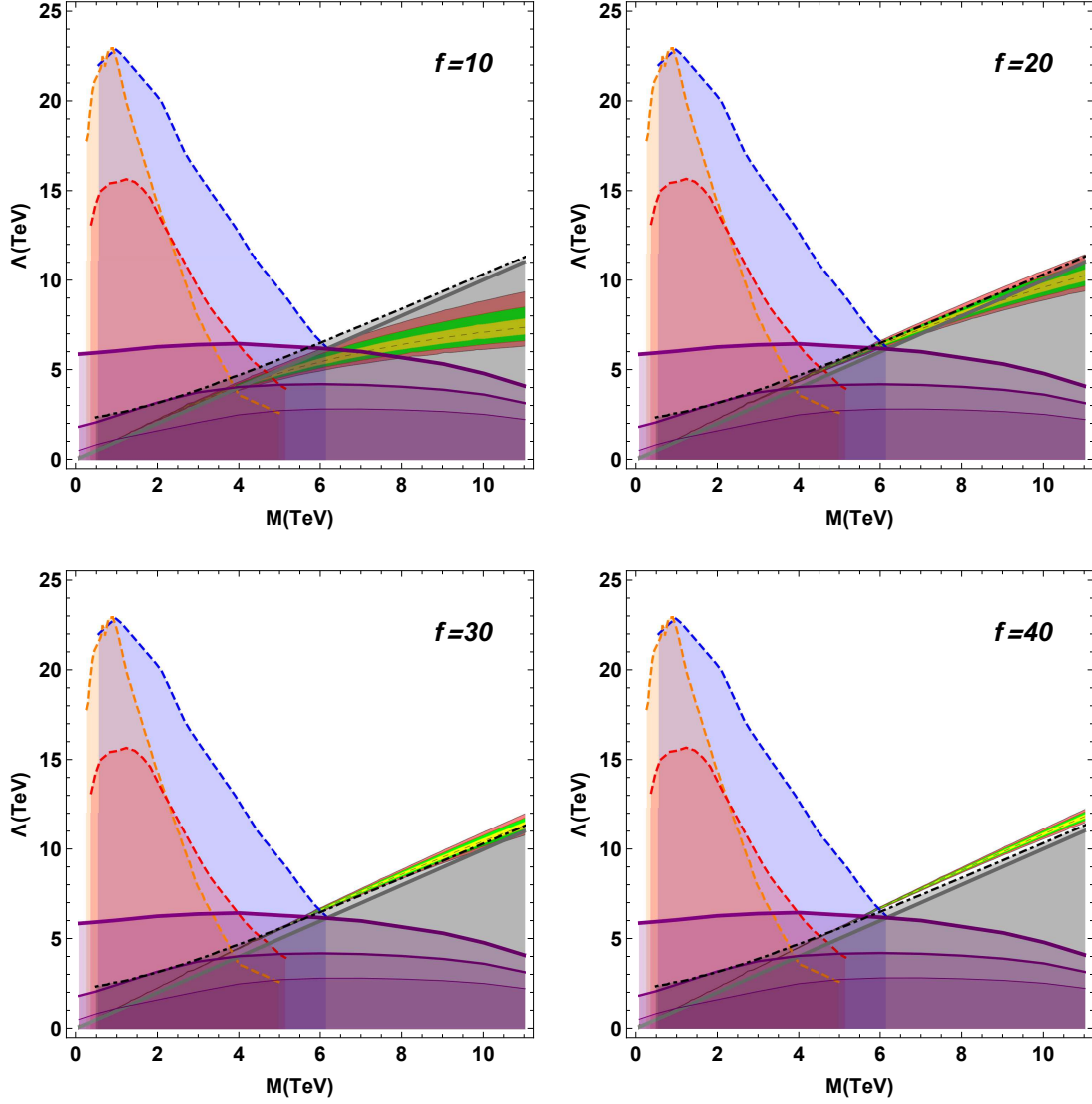


Figure 6: $\Delta a_\mu^{\text{Exc}}$ in (M, Λ) plane for the case of excited lepton doublet including the exclusions from $\Delta\rho$ due to non-degenerate excited fermions with $\delta M = 15$ GeV (dotted-dashed black line). The upper-left (upper-right) plot corresponds to the value of weight factor $f = 10$ ($f = 20$) whereas the lower-left (lower-right) plot correspond to the value $f = 30$ ($f = 40$). Other lines and color coding remain same as in previous figures.

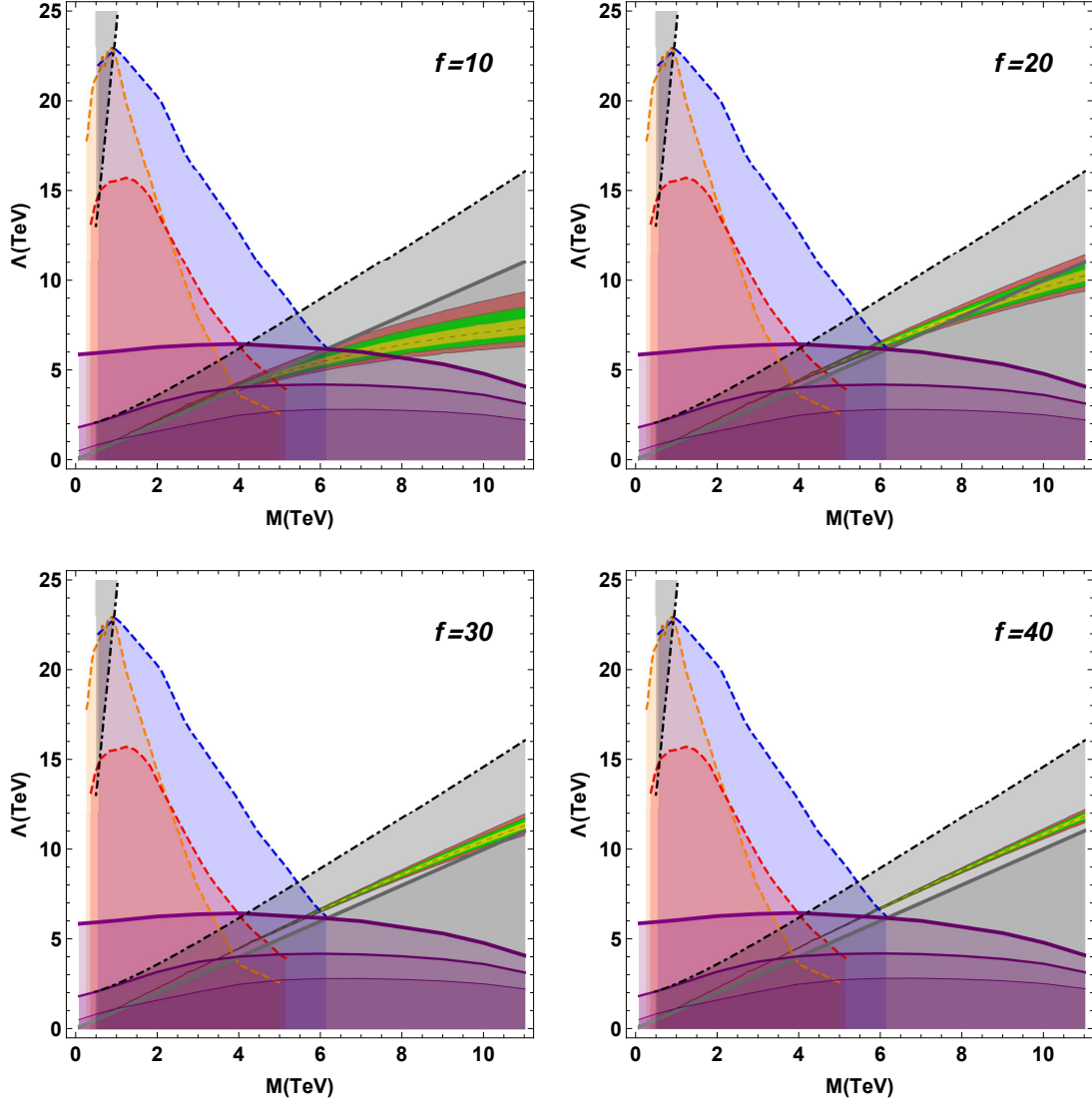


Figure 7: $\Delta a_{\mu}^{\text{Exc}}$ in (M, Λ) plane for the case of excited lepton doublet including the exclusions from $\Delta\rho$ due to non-degenerate excited fermions with $\delta M = 20$ GeV (dotted-dashed black line). The upper-left (upper-right) plot corresponds to the value of weight factor $f = 10$ ($f = 20$) whereas the lower-left (lower-right) plot correspond to the value $f = 30$ ($f = 40$). Other lines and color coding remain same as in previous figures.

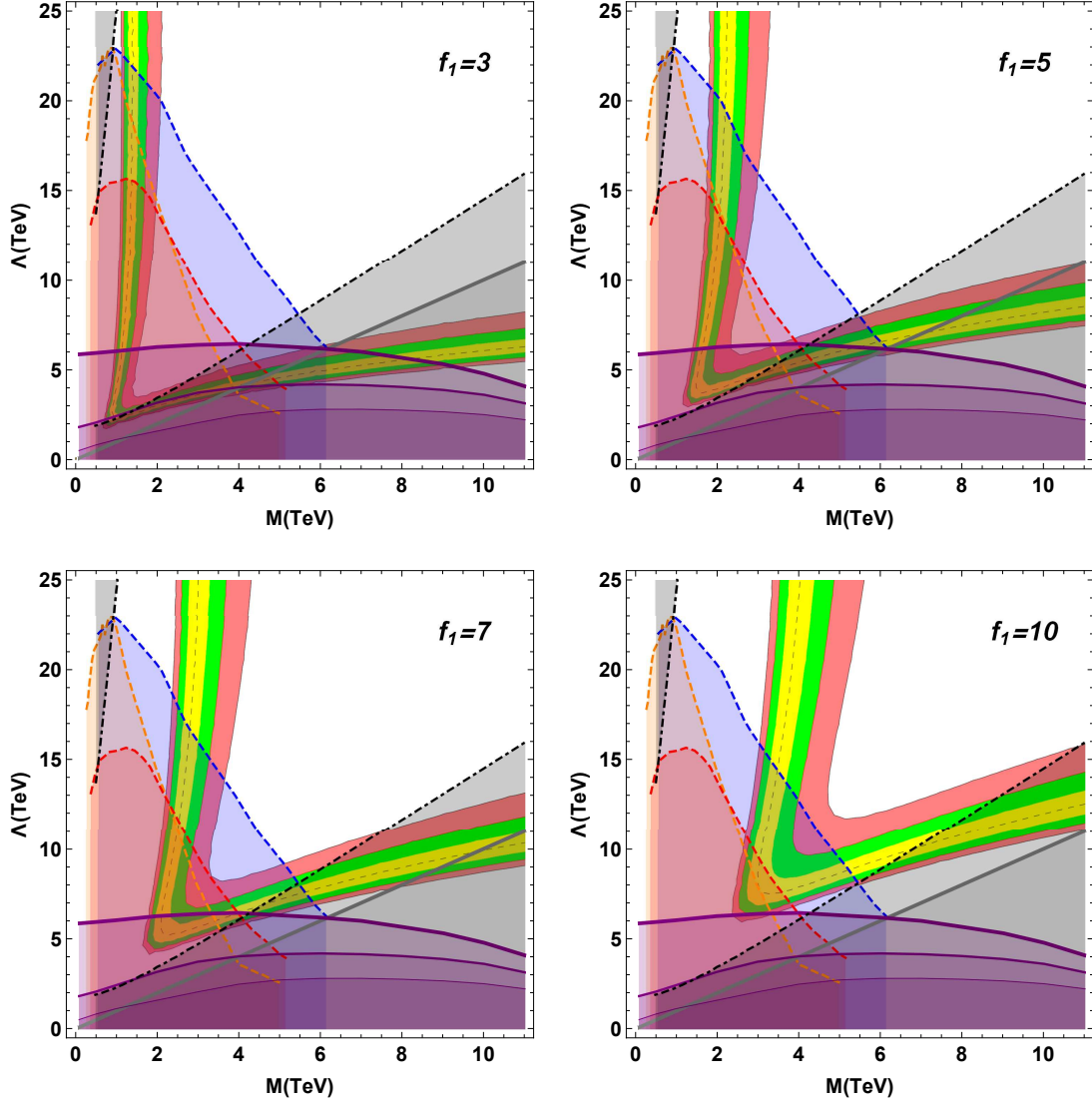


Figure 8: $\Delta a_{\mu}^{\text{Exc}}$ in (M, Λ) plane for the case of excited lepton triplet including the exclusions from $\Delta\rho$ due to non-degenerate excited fermions with $\delta M = 10$ GeV (dotted-dashed black line). The upper-left (upper-right) plot corresponds to the value of weight factor $f_1 = 3$ ($f_1 = 5$) whereas the lower-left (lower-right) plot correspond to the value $f_1 = 7$ ($f_1 = 10$). Other lines and color coding remain same as in previous figures.

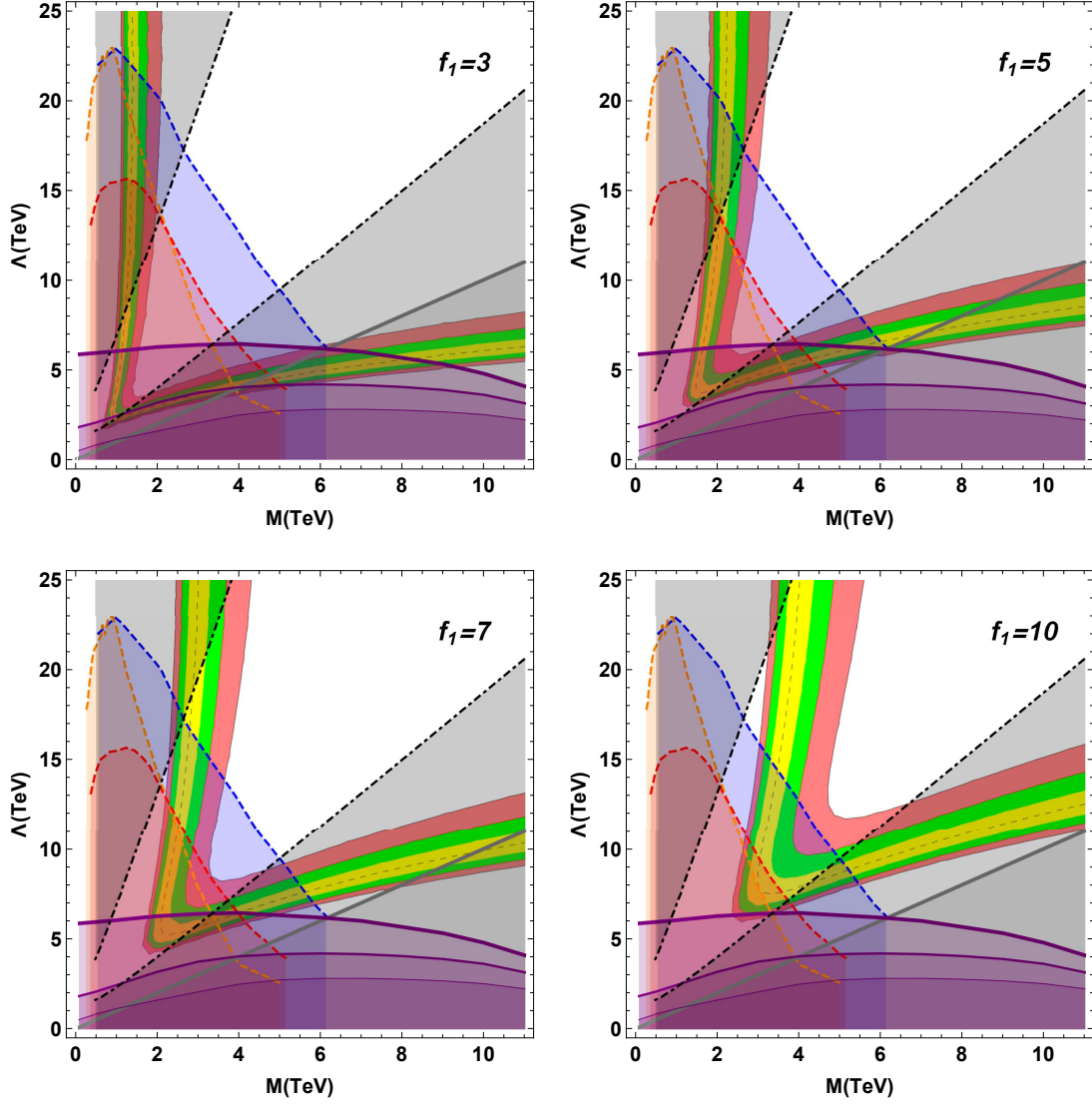


Figure 9: $\Delta a_\mu^{\text{Exc}}$ in (M, Λ) plane for the case of excited lepton triplet including the exclusions from $\Delta\rho$ due to non-degenerate excited fermions with $\delta M = 15$ GeV (dotted-dashed black line). The upper-left (upper-right) plot corresponds to the value of weight factor $f_1 = 3$ ($f_1 = 5$) whereas the lower-left (lower-right) plot correspond to the value $f_1 = 7$ ($f_1 = 10$). Other lines and color coding remain same as in previous figures.

5 Conclusions

The latest measurements of the muon’s magnetic moment, $(g - 2)_\mu$, conducted by the Muon $g - 2$ collaboration at Fermilab [1, 2], reaffirm that the predictions of the Standard Model (SM) for $(g - 2)_\mu$ are insufficient. They indicate the necessity of incorporating new physics effects to align with the experimental findings.

In our previous work, we illustrated the strong correlation between the prediction for $\Delta\rho$ and the non-degeneracy in mass between excited lepton doublets and triplets. Conversely, the computation of $(g - 2)_\mu$ remains unaffected by mass non-degeneracy. Thus, we explored two scenarios: the degenerate scenario, where constraints from $\Delta\rho$ are irrelevant, and non-degenerate scenario where the model’s parameter encounters significant constraints due to $\Delta\rho$.

We initially examined the predictions of $(g - 2)_\mu$ in the excited fermion model, considering higher isospin multiplets with degenerate masses, and setting $f' = f$. The doublet and triplet contributions are sensitive to the value of weight factors f' , f and f_1 and show only mild dependence on the weight factor k . For the case of isospin doublet contributions, we found that the required value of $(g - 2)_\mu$ can only be obtained in the area that is already excluded by other constraints except for value of weight factor $f > 20$.

In contrast, the observed deviation in $(g - 2)_\mu$ can be effectively accounted for by contributions from isospin triplets. These contributions are notably significant compared to the doublet contributions for equivalent values of the weight factor f_1 . Moreover, the required $(g - 2)_\mu$ value can be attained within the allowed (M, Λ) region for relatively smaller f_1 values. The doublet and triplet contributions to the $(g - 2)_\mu$ impose stringent constraints on the parameter space of the excited fermion model, surpassing those from experimental searches and perturbative unitarity bounds.

As a subsequent step, we explored the possibility where $f' \neq f$. Since only f_1 affects triplet contributions, the results remain unaffected in the triplet case. However, for doublets, introducing a negative value for f' can lead to significant changes. In this scenario, doublet contributions can also accommodate the $(g - 2)_\mu$ anomaly within the allowed range of parameter space, with small values for both f' and f .

We also explored the model parameter space for the case of non-degenerate masses, incorporating constraints from experimental searches, unitarity bounds, electroweak precision observable $\Delta\rho$, and $(g - 2)_\mu$. As was reported earlier, a significant portion of the (M, Λ) plane is invalidated by $\Delta\rho$ when the masses are non-degenerate. Consequently, the $(g - 2)_\mu$ anomaly cannot be accounted for if the mass difference between the excited fermions, denoted by δM , exceeds 15 GeV for excited fermion doublets and 10 GeV for excited fermion triplets.

Acknowledgments

The research of M. E. G. is supported by the Spanish MICINN, under grant PID2022-140440NB-C22. The research of O. P. is supported by the Istituto Nazionale di Fisica Nucleare, under the grant: “Exploring New Physics” (ENP).

References

- [1] D. P. Aguillard *et al.* [Muon g-2], Phys. Rev. Lett. **131** (2023) no.16, 161802 [arXiv:2308.06230 [hep-ex]].
- [2] B. Abi *et al.* [Muon g-2], Phys. Rev. Lett. **126** (2021) no.14, 141801 [arXiv:2104.03281 [hep-ex]].
- [3] G. W. Bennett *et al.* [Muon g-2], Phys. Rev. D **73** (2006), 072003 [arXiv:hep-ex/0602035 [hep-ex]].
- [4] T. Aoyama, N. Asmussen, M. Benayoun, J. Bijnens, T. Blum, M. Bruno, I. Caprini, C. M. Carloni Calame, M. Cè and G. Colangelo, *et al.* Phys. Rept. **887** (2020), 1-166 [arXiv:2006.04822 [hep-ph]].
- [5] U. Baur, M. Spira and P. M. Zerwas, Phys. Rev. D **42** (1990), 815-824
- [6] U. Baur, I. Hinchliffe and D. Zeppenfeld, Int. J. Mod. Phys. A **2** (1987), 1285
- [7] G. Aad *et al.* [ATLAS], Phys. Rev. Lett. **105** (2010), 161801 [arXiv:1008.2461 [hep-ex]].
- [8] G. Aad *et al.* [ATLAS], JHEP **02** (2016), 110 [arXiv:1510.02664 [hep-ex]].
- [9] M. C. Gonzalez-Garcia and S. F. Novaes, Nucl. Phys. B **486** (1997), 3-22 [arXiv:hep-ph/9608309 [hep-ph]].
- [10] G. Pancheri and Y. N. Srivastava, Phys. Lett. B **146** (1984), 87-94
- [11] S. Biondini, O. Panella, G. Pancheri, Y. N. Srivastava and L. Fano, Phys. Rev. D **85** (2012), 095018 [arXiv:1201.3764 [hep-ph]].
- [12] R. Leonardi, O. Panella and L. Fanò, Phys. Rev. D **90** (2014) no.3, 035001 [arXiv:1405.3911 [hep-ph]].
- [13] S. Biondini and O. Panella, Phys. Rev. D **92** (2015) no.1, 015023 [arXiv:1411.6556 [hep-ph]].
- [14] R. Leonardi, L. Alunni, F. Romeo, L. Fanò and O. Panella, Eur. Phys. J. C **76** (2016) no.11, 593 [arXiv:1510.07988 [hep-ph]].
- [15] A. M. Sirunyan *et al.* [CMS], JHEP **04** (2019), 015 [arXiv:1811.03052 [hep-ex]].
- [16] A. Tumasyan *et al.* [CMS], Phys. Lett. B **843** (2023), 137803 [arXiv:2210.03082 [hep-ex]].
- [17] G. Aad *et al.* [ATLAS], JHEP **06** (2023), 199 [arXiv:2303.09444 [hep-ex]].
- [18] S. Biondini, R. Leonardi, O. Panella and M. Presilla, Phys. Lett. B **795** (2019), 644-649 [erratum: Phys. Lett. B **799** (2019), 134990] [arXiv:1903.12285 [hep-ph]].

- [19] M. Rehman, M. E. Gomez and O. Panella, Eur. Phys. J. C **81** (2021) no.5, 392 [arXiv:2010.01808 [hep-ph]].
- [20] S. J. Brodsky and S. D. Drell, Phys. Rev. D **22** (1980), 2236
- [21] F. M. Renard, Phys. Lett. B **116** (1982), 264-268
- [22] M. C. Gonzalez-Garcia and S. F. Novaes, Phys. Lett. B **389** (1996), 707-712 [arXiv:hep-ph/9609393 [hep-ph]].
- [23] F. Boudjema, A. Djouadi and J. L. Kneur, Z. Phys. C **57** (1993), 425-450
- [24] K. Hagiwara, D. Zeppenfeld and S. Komamiya, Z. Phys. C **29** (1985), 115
- [25] S. P. Martin and J. D. Wells, Phys. Rev. D **64** (2001), 035003 [arXiv:hep-ph/0103067 [hep-ph]].
- [26] F. V. Ignatov *et al.* [CMD-3], [arXiv:2309.12910 [hep-ex]].
- [27] D. P. Aguillard *et al.* [Muon g-2], [arXiv:2402.15410 [hep-ex]].